N. A. E.

R. & M. No. 2697
(12,455)
A.R.C. Technical Report

MINISTRY OF SUPPLY

AERONAUTICAL RESEARCH COUNCIL
REPORTS AND MEMORANDA

Some High-Speed Tests on Turbine Cascades

By

E. A. Bridle, B.Sc., D.I.C.

LONDON: HER MAJESTY'S STATIONERY OFFICE

1953

FOUR SHILLINGS NET

Some High-Speed Tests on Turbine Cascades

By

E. A. BRIDLE, B.Sc., D.I.C.

COMMUNICATED BY THE PRINCIPAL DIRECTOR OF SCIENTIFIC RESEARCH (AIR), MINISTRY OF SUPPLY

Reports and Memoranda No. 2697

February, 1949

Summary.—High-speed wind-tunnel tests on seven cascades of turbine blades are described, the blades having conventional sections including both reaction and impulse designs. The two-dimensional performance over wide ranges of incidence at Mach numbers up to 1·0 is discussed, special importance being attached to the effects of compressibility.

It is shown that the effect of increasing the degree of reaction is to reduce the total-head loss and to increase the unstalled incidence range. High Mach numbers alone are not found to cause a catastrophic increase in loss with these particular blade designs, while the $\cos^{-1}$ throat/pitch rule is found to be approximately true only at high Mach numbers.

1. *Introduction.*—The design of turbines and the estimation of their performance is, at present, based largely on experience and on the results of low-speed tests on cascades of aerofoils[1, 2]. There is, however, little information concerning the behaviour of turbine blades under the conditions which obtain in an engine.

This report describes some high-speed tests carried out on a number of turbine cascades in order,

(a) to investigate the effect of compressibility on the two-dimensional performance of different turbine blade sections,

and (b) to discover the combinations of blade and air angles with which efficient operation may be expected.

2. *Notation.*—The notation used conforms to that of R. & M. 2095[3] with some exceptions which are explained in the text where necessary. A list of all the quantities involved is given in an Appendix, while the cascade notation is also given in Fig. 3.

3. *Description of Wind Tunnel.*—The cascades were tested in High-Speed Cascade Wind Tunnel No. 3, which is illustrated in Fig. 1. It is of the open-jet type, discharging to atmosphere with no restricting walls after the cascade. Boundary-layer suction is not applied, as the number of blades, *viz.*, thirteen, is considered large enough to ensure an approach to two-dimensional conditions in the middle of the cascade. Air is supplied to the tunnel by a multi-stage centrifugal compressor.

3.1. *Construction.*—From the air delivery pipe, the cross-section is reduced to a rectangle through a cast light alloy accelerator, and thence by means of a light alloy adaptor to one of a series of welded mild steel tunnel ends. These are interchangeable, and are chamfered to give air inlet angles to the cascades from 0 deg to 70 deg at 5 deg intervals. The overall contraction ratio up to the cascade varies from 5 : 1 to 15 : 1 depending on which tunnel end is used, the latter being designed for a fixed cascade length of 7·5 in. and a blade height of 2·0 in.

The cascades are of mild steel, and each set of blades is located in shrouds by dowels, with 7·5 in. between the extreme blades. They are bolted to angle sections which slide in grooves machined in the tunnel ends. This ensures a smooth joint between the tunnel end and the blade shrouds, and enables the leaving edges of the extreme blades to be aligned with the tunnel walls.

The downstream measuring instrument is manipulated by a system of lead-screws, which enables a traverse to be made over all the blades at any blade height and at different distances from the cascade. The instrument can be rotated, for measuring air direction, by a slow-motion drive. The screw system is supported by a cast light alloy ring, and can be rotated so that it is parallel to any tunnel end. The complete traversing mechanism is mounted on one side of the accelerator casting, and can be fitted to either side for calibration purposes.

3.2. *Instrumentation and Calibration.*—A total-head tube located upstream of the accelerator is used as a datum when maintaining a given pressure ratio across the tunnel. The total-head pressure at inlet to the cascade is measured by a pitot-tube which can be traversed at mid-blade height upstream of the cascade and removed during downstream traversing. The inlet static pressure is measured immediately upstream of the cascade by means of a number of tappings flush with the tunnel walls. For normal downstream measurement a combined pitot-tube and yawmeter of the claw type shown in Fig. 1 is traversed one blade chord downstream of the cascade.

Traverses over the open tunnel ends, *i.e.*, with no cascade, were made at different Mach numbers and indicated a uniform total-head distribution in all cases, results for one tunnel end being given in Fig. 2. Further traverses were made with a $\frac{1}{2}$-in. diameter windmill with untwisted vanes and there was found to be complete absence of vorticity except in the extreme corners of the tunnel ends, where the windmill rotated rapidly.

The direction of airflow in each tunnel end was found from two sets of yawmeter readings, which were taken with the traversing gear on different side of the tunnel to eliminate any zero error in the instrument. The deviation from the axial direction was found to be within $\pm \frac{1}{2}$ deg for all the tunnel ends and was independent of Mach number. The zero error of the yawmeter was also calculated from the above readings.

With the cascades in position, total-head traverses at mid-blade height showed good agreement between successive wakes, and a typical result for one cascade is shown in Fig. 2. A traverse over only two blades was found to give an accurate value of the mean total head. The corresponding upstream static-pressure readings showed a small random variation between different tappings, which was probably due to their being in the boundary layer. This introduced an error of the order of $\pm$ 1 per cent into the estimated inlet Mach numbers.

4. *Cascade Aerodynamic Details.*—Full dimensions of the cascades are given in Fig. 4 and the blade sections are illustrated in Fig. 5. Seven cascades were tested, and these comprised

(a) a series of four designed for a constant outlet angle with different blade inlet angles (Cascades Nos. 1, 2, 3 and 4),

(b) two cascades designed for the same inlet angle with different outlet angles (Cascades Nos. 4 and 7),

(c) a series of three impulse-type cascades designed for different deflections (Cascades Nos. 1, 5 and 6).

The ratio (s/w) of blade pitch to cascade axial width was the same for all cascades, namely, 0·625.

4.1. *Design Data.*—The blades had conventional turbine sections, as distinct from aerofoils, being designed arbitrarily from two and three circular-arcs with a straight line upper surface to the trailing edge giving a throat at outlet. The leading edges were radiused and the trailing edges were given a chamfer of constant width parallel to the cascade, as shown in Fig. 4. It will be seen that there was a random variation in leading-edge radius from cascade to cascade, and that the trailing-edge thickness depended on the outlet angle. These discrepancies were caused by the designs being based on geometrical formulae rather than on aerodynamic principles. Leading and trailing-edge dimensions were, therefore, functions of blade angles and pitch, not of

maximum blade thickness and chord as might be expected. For the same reason, the ratio (t/c) of maximum-blade-thickness to chord increased with camber and outlet angle. The extent of the latter variation can be seen in Fig. 5.

The design inlet angle (α_{1D}) for zero incidence was defined to bisect the directions of the upper and lower surfaces where they touched the leading-edge circle (*see* Fig. 3). The outlet angle was designed, from existing information on nozzles, in accordance with the approximate rule.

$$\alpha_2 = \cos^{-1}\frac{A_t}{S}. \qquad (1)$$

4.2. *Aerofoil Classification.*—For general cascade investigations it is useful to define turbine blades in a similar manner to the aerofoils used for compressor blades, as this aids correlation of the two.

An attempt was made to reduce the seven blade sections to a single-base profile, designated 'T6'[4], the cascades then being expressed in terms of it. The results closely approximated to the original sections and are tabulated below. The notation is similar to that used in R. & M. 2095[3]. For example, Cascade No. 5 is defined by

$$21{\cdot}7\ \text{T6}/91{\cdot}3\ \text{P}\ 43{\cdot}5\,,$$

where 21·7 is the maximum thickness (t) as a percentage of the chord (c); T6 is the base profile; 91·3 is the camber (θ) in degrees; P denotes that the camber-line bisecting the blade section is a parabolic-arc; and 43·5 is the distance (a) of the position of maximum camber from the leading edge as a percentage of the chord.

Cascade	Aerofoil	ξ	S/C	β_1	β_2
1	31·3 T6/110·5 P 41·7	+ 8·6	0·627	55·4	−55·1
2	28·35 T6/102 P 41·8	+14·0	0·613	46·0	−56·0
3	23·55 T6/92·5 P 41·3	+21·5	0·584	35·5	−57·0
4	18·08 T6/76·8 P 40·8	+28·5	0·551	18·8	−58·0
5	21·7 T6/91·3 P 43·5	+ 9·0	0·625	45·5	−45·8
6	14·75 T6/74 P 44·5	+ 6·3	0·627	36·7	−37·3
7	15·15 T6/66 P 42·2	+21·2	0·584	18·9	−47·1

The blade angles (β_1, β_2) under aerofoil classification are defined by the directions of the superimposed parabolic-camber line at the leading and trailing edges, and differ from the design values, making it rather difficult to define the angles of incidence and deviation. The parabolic camber-line is, however, an approximation and it is considered reasonable to measure incidence with respect to α_{1D} thus

$$i = \alpha_1 - \alpha_{1D} \qquad (2)$$

which is not in strict agreement with the notation of R. & M. 2095[3]. On the other hand, $\cos^{-1} A_t/S$ does not correspond to any mean blade angle, and deviation will be measured from the camber-line, thus

$$\delta = \alpha_2 - \beta_2\,. \qquad (3)$$

5.0. *Presentation of Test Results.*—In Figs. 6 to 12 the mean air outlet angle, static-pressure drop and total-head loss are plotted against outlet Mach number. This Mach number is a mean value, $\bar{M}_2$, calculated from the ratio of the mean outlet total-head pressure, $P_{\text{tot}2}$, to the static pressure, P_2, and is given by the general equation

$$\frac{P_{\text{tot}}}{P} = \left\{1 + \frac{\gamma - 1}{2}\,.\,M^2\right\}^{\gamma/(\gamma-1)}. \qquad (4)$$

It will be seen from equation (4) that the overall total-head to static-pressure ratio, P_{tot}/P_2, gives the theoretical outlet Mach number, M_{2th}, obtained with no loss. The ratio $\bar{M}_2/M_{2th}$ is then equal to $\bar{V}_2/V_{2th}$, the velocity coefficient used in steam turbine practice.

The total head loss, $\bar{\omega}$, and static-pressure drop, ΔP, are expressed in terms of $P_{tot1} - P_2$, the theoretical outlet dynamic head obtained with no loss. The static-pressure-drop coefficient is then equal to unity when the inlet velocity is zero, *i.e.*, $P_{tot1} = P_1$, and equal to zero under impulse conditions, becoming negative when there is a rise in pressure through the cascade.

The values of air inlet angle, α_1, shown on the curves are given to the nearest degree, to avoid confusion. The exact values differ from whole numbers by up to $\frac{1}{2}$ deg, due to the tunnel effect discussed in section 3.2.

Fig. 13 shows the variation of inlet Mach number, M_1, with the flow area ratio for constant mean outlet Mach numbers up to unity. The flow area ratio is equal to $\cos \alpha_2/\cos \alpha_1$ and with no loss it is a function of M_1 and M_2 only, being given by the following equation, which has been derived elsewhere[3] :—

$$\frac{\cos \alpha_2}{\cos \alpha_1} = \frac{M_1}{M_2}\left(\frac{1 + \frac{\gamma - 1}{2} \cdot M_2^2}{1 + \frac{\gamma - 1}{2} \cdot M_1^2}\right)^{\frac{1}{2} \cdot \frac{\gamma + 1}{\gamma - 1}} \quad \ldots \quad (5)$$

It should be emphasized that in this continuity equation $\cos \alpha_2$ is proportional to the outlet flow area and does not correspond to the throat area of the cascade. The inlet Mach number is calculated from equation (4) by substituting the ratio P_{tot1}/P_1. Each curve includes the results for all seven cascades, interpolated from Figs. 6 to 12. These derived points are shown on the curves for $\bar{M}_2 = 0{\cdot}3$, $0{\cdot}6$ and $1{\cdot}0$. The points at which impulse conditions, *i.e.*, $\Delta P = 0$, were obtained are also plotted in Fig. 13. The theoretical curve for an outlet Mach number of unity is shown for comparison, being calculated from equation (5) with $\gamma = 1{\cdot}4$, the equation becoming

$$\frac{\cos \alpha_2}{\cos \alpha_1} = 1{\cdot}728 M_1 (1 + 0{\cdot}2 M_1^2)^{-3} . \quad \ldots \quad (6)$$

In Fig. 14 the total-head loss of the three impulse-type cascades is plotted against both deflection and flow area ratio for a mean outlet Mach number of $1{\cdot}0$. The curves are obtained by extrapolation from Figs. 6, 10 and 11, deflection being given by

$$\varepsilon = \alpha_1 - \alpha_2 . \quad \ldots \quad (7)$$

6. *Discussion.*—The lack of uniformity in design prevents any systematic analysis of the test results, but it is possible, nevertheless, to note certain phenomena which are common to all the cascades. It may be remarked that they are representative of the type of blading largely used in actual gas turbines, and the test results can, therefore, be expected to have practical significance.

With the type of atmospheric wind tunnel used for the tests it was not possible to vary the Mach number independently of Reynolds number, the two quantities being connected by the approximate relationship

$$R = M_2 \times 3{\cdot}0 \times 10^5 \quad \ldots \quad (8)$$

where Reynolds number is based on blade chord and outlet velocity. The effects of Reynolds number and Mach number, however, are most predominant at the low and high-speed ends of the range respectively, so that some specific conclusions may be drawn about each.

An effect which is common to all the cascades is an increase in total-head loss at low Mach or Reynolds numbers. This is undoubtedly due to the increase in form drag when the boundary layer is mainly laminar[5] and unable to negotiate the adverse static-pressure gradient at the rear of the upper blade surface. The effect is much less pronounced with the higher degrees of

reaction when, presumably, the more favourable conditions delay separation of the boundary layer. Over this low-speed range both the air outlet angle and the static-pressure-drop coefficient remain fairly constant, and the inlet Mach number is found to increase almost linearly with outlet Mach number at a given incidence.

Another common feature is an increase in loss which occurs when the outlet Mach number exceeds about 0·7. The loss reaches a maximum at a Mach number between 0·8 and 0·9, any further increase in Mach number resulting in a decrease in loss. It has been shown by Todd[6] that the initial increase in loss is associated with the formation of a shock system on the rear upper surface of the blade, interaction between the shock system and the boundary layer causing turbulent separation of the latter. Furthermore, Todd has shown that as the Mach number is increased, the base of the shock and hence the point of separation move back towards the trailing edge, with the consequent fall in loss remarked above. In fact, the smallest loss at a given incidence may occur when the cascade is ' choked ' at outlet and the shock system has reached its rearmost position. These effects can be very pronounced, as shown, for example, by the impulse cascade results of Fig. 10, when steep opposing pressure gradients encourage detachment of the boundary layer. On the other hand, the effects are hardly noticeable in the results for the reaction cascade shown in Fig. 9.

The increase in loss referred to above is accompanied by an increase in the air outlet angle, and hence in deflection, which would not be expected from the worsened condition of the boundary layer. The effect is presumably due to the shock system noted above, but the exact mechanism is not yet clear. At the higher Mach numbers the air outlet angle approaches the well-known value of $\cos^{-1}$ (throat/pitch), though it is often less than this value by up to 3 deg. At lower Mach numbers the difference is even greater, and the use of the theoretical value could introduce large errors. On the other hand, $\cos^{-1}$ (throat/pitch) appears to form a better basis for comparison than the mean backbone angle, α_2, the use of which can involve both positive and negative deviations in the unstalled condition. The variation of air outlet angle with incidence is very small, unless the cascade is shock stalled, and at a given Mach number only amounts to some 3 deg over the whole range covered.

The increase in air outlet angle at high Mach number affects the degree of reaction, and there is a corresponding increase in static-pressure drop. At a given incidence and outlet Mach number, this results in a lower inlet Mach number than would be expected were no shock system present, and the inlet Mach number tends towards a maximum as the outlet Mach number approaches unity. The relationship between inlet and outlet Mach numbers is clearly a function of the flow area ratio, $\cos \alpha_2/\cos \alpha_1$, as shown in Fig. 13, where the three quantities are plotted as a series of general curves. The scatter of the points is due to differences in loss between the cascades. Theoretically, with a flow area ratio of unity, the inlet and outlet Mach numbers would be equal and impulse conditions would obtain. In practice, however, this latter condition is only obtained with a flow area ratio exceeding unity, owing to the existence of losses.

A more particular effect is an increase in loss at quite low Mach numbers, often followed by a decrease as shown in Fig. 11, for example. This generally seems to occur at an inlet Mach number of about 0·5, and suggests the possible formation of a shock system near the leading edge of the blade. With the higher degrees of reaction the inlet Mach number never reaches 0·5 and there is no apparent increase in loss. In the case of blades operating at or near impulse conditions, however, and especially when there is an overall rise in static pressure across the cascade, the loss may become very great. This type of blade, moreover, is often required to work with a high inlet Mach number, and a limit must, therefore, be put on the air inlet angle if high losses are to be avoided. The tests indicate that flow area ratio is a useful criterion and that, generally speaking, a value of 1·0 should not be exceeded. In other words, numerically, the gas inlet angle should always be less than the gas outlet angle. This is well illustrated in Fig. 14, where a sharp increase in loss is seen to occur in each case as the area ratio is increased about unity, whereas incidences are only of the order of 5 deg to 10 deg. Referring again to Fig. 13, this is seen to limit the inlet Mach number to about 0·75 when the cascade is choked.

Further inspection of Figs. 6 to 12 reveals that with a high degree of reaction, a low loss can be obtained over a wide incidence range. An approach to impulse conditions results in a considerable increase in unstalled loss and a smaller permissible range of incidence, especially at low Mach numbers.

7. *Conclusions.*—It will be realised that the tests which have been described are by no means exhaustive, but should nevertheless provide a useful guide to the estimation of turbine performance. As far as it is possible to generalize, the following points are worth noting :—

(a) Increasing the degree of reaction reduces the total-head loss and increases the unstalled incidence range. Impulse blades can be expected to give high losses, but these do not become prohibitive unless the gas inlet angle exceeds that at exit from the blades.

(b) High Mach numbers alone do not cause a catastrophic increase in loss, the exact variation depending on the geometry of the blading.

(c) At high Mach numbers the $\cos^{-1}$ (throat/pitch) rule for outlet angle is only approximately true, and wide differences may be expected at lower Mach numbers.

REFERENCES

No.	*Author*	*Title, etc.*
1	J. Reeman	The Turbine for the Simple Jet Propulsion Engine. *Proc. Inst. Mech. E.*, 1945, Vol. 153 (War Emergency Issue No. 12).
2	J. Reeman	Performance of Cascades of Aerofoils at Positive Stagger. Power Jets Memorandum No. M.1203. March, 1946. A.R.C. 10,829. (Unpublished.)
3	A. R. Howell	The Present Basis of Axial Flow Compressor Design. Part I. Cascade Theory and Performance. R. & M. 2095. 1942.
4	M. Mettam	Turbine Blade Section T6. Power Jets Memorandum No. M.1081. April, 1945.
5	S. Goldstein	*Modern Developments in Fluid Dynamics.* Vol. 1, Ch. II. Oxford University Press. 1943.
6	K. W. Todd	Practical Aspects of Cascade Wind Tunnel Research. *Proc. Inst. Mech. E.*, 1947, Vol. 157 (War Emergency Issue No. 36).

APPENDIX

Notation

a	Distance of position of maximum camber from leading edge
c	Chord
i	Incidence
r_1	Leading-edge radius
s	Pitch
t	Maximum thickness
w	Cascade axial width
A	Flow area
A_t	Throat area
L.E.	Leading edge
M	Mach number
$\bar{M}$	Mean Mach number
P	Static pressure
P_{tot}	Total-head pressure
R	Reynolds number
V	Velocity
α	Air angle
α_D	Design angle
β	Blade angle (aerofoil classification)
γ	Ratio of specific heats
δ	Deviation
ε	Deflection
ζ	Stagger
θ	Camber
$\bar{\omega}$	Mean total-head loss
ΔP	Static-pressure drop

Suffix 1 refers to inlet conditions to the cascade

Suffix 2 refers to outlet conditions from the cascade

Suffix 'th' refers to theoretical quantities

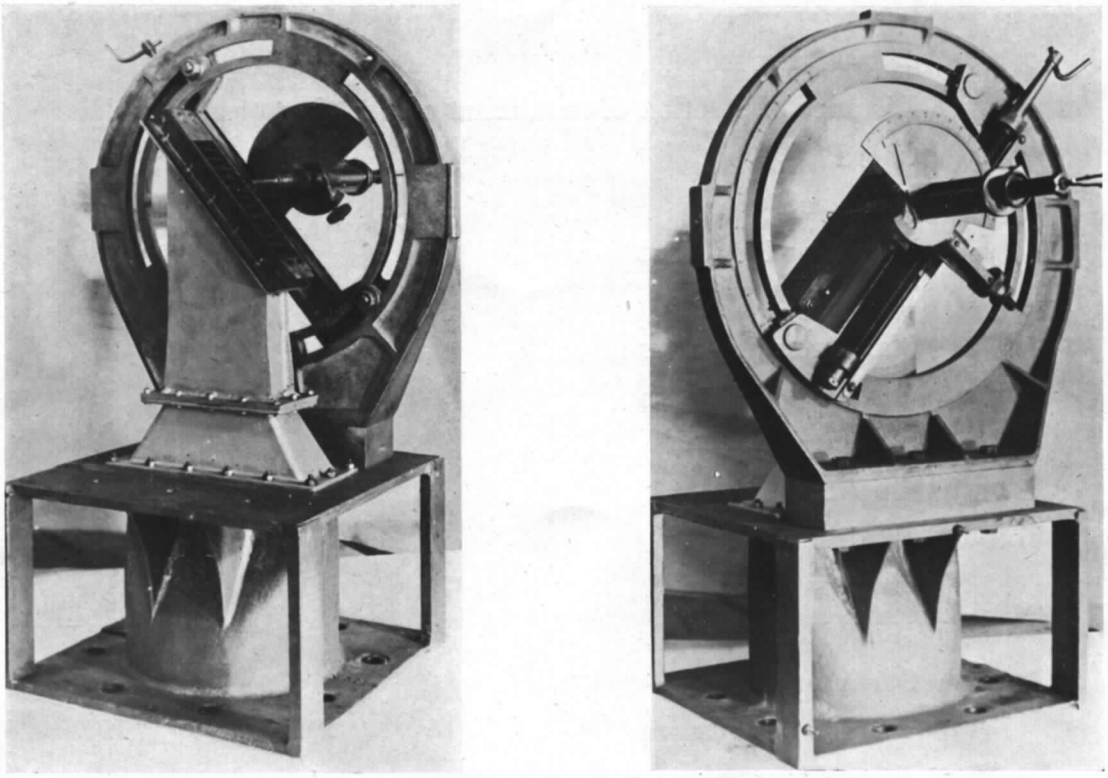

FIG. 1. High-Speed Cascade Tunnel No. 3.

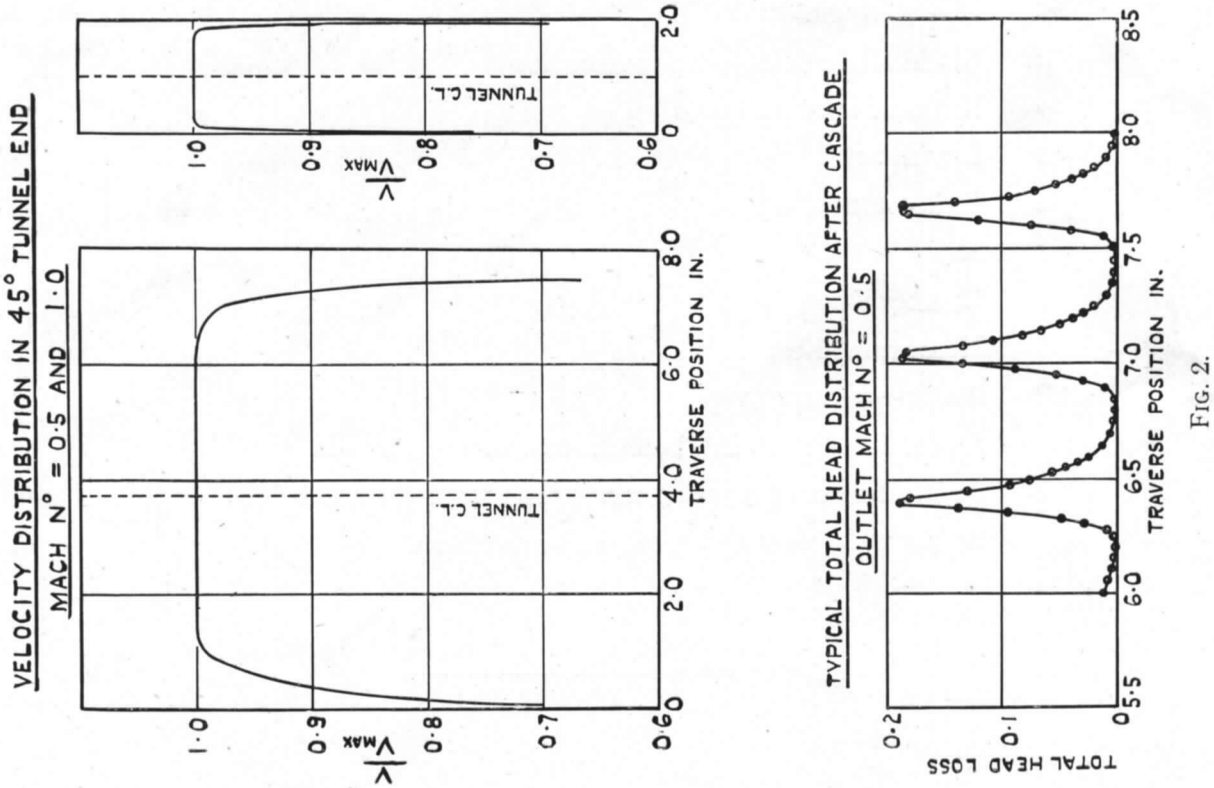

FIG. 2.

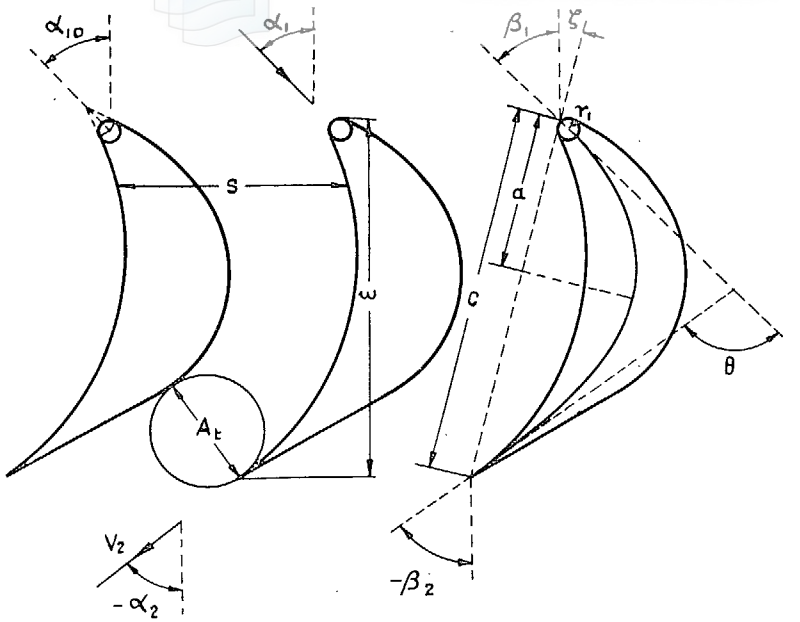

a	POSITION OF MAXIMUM CAMBER FROM L.E.
c	CHORD
r_1	L.E. RADIUS
s	PITCH
ω	WIDTH = c x cos ζ
A_t	THROAT AREA
V_1	AIR INLET VELOCITY
V_2	AIR OUTLET VELOCITY
α_1	AIR INLET ANGLE
α_2	AIR OUTLET ANGLE
α_{10}	DESIGN INLET ANGLE
β_1	BLADE INLET ANGLE (AEROFOIL NOTATION)
β_2	BLADE OUTLET ANGLE(" ")
ζ	STAGGER
i	INCIDENCE = $\alpha_1 - \alpha_{10}$
δ	DEVIATION = $\alpha_2 - \beta_2$
θ	CAMBER = $\beta_1 - \beta_2$

FIG. 3. Cascade notation.

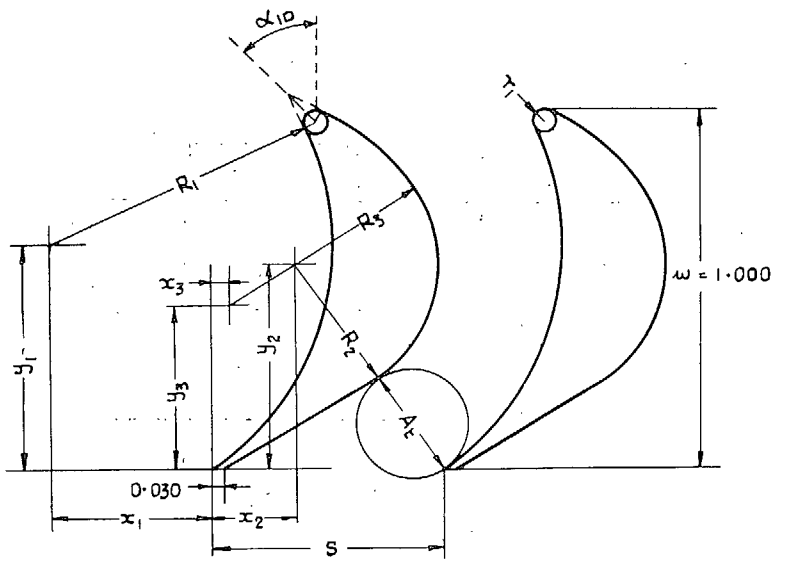

CASCADE N°	1 *	2	3	4	5 *	6 *	7
s/ω	0·625	0·625	0·625	0·625	0·625	0·625	0·625
$\alpha_{1\,0}$	55°	45°	30°	15°	45°	35°	15°
$\cos^{-1} A_t/s$	-60°	-60°	-60°	-60°	-50°	-40°	-50°
x_1	0·389	0·439	0·555	0·717	0·598	0·838	0·902
x_2	0·236	0·226	0·189	0·138	0·027	-0·213	-0·079
x_3	0·051	0·049	0·092	-	-	-	-
y_1	0·556	0·626	0·791	1 024	0·598	0·586	0·902
y_2	0·556	0·570	0·623	0·696	0·598	0·586	0·704
y_3	0·426	0·457	0·561	-	-	-	-
R_1	0·679	0·765	0·966	1·251	0·846	1·023	1·276
R_2	0·366	0·384	0·448	0·537	0·440	0·547	0·594
R_3	0·592	0·594	0·563	-	-	-	-
r_1	0·035	0·035	0·035	0·032	0·032	0·025	0·040

* CONSTANT PASSAGE AREA

FIG. 4. Cascade details.

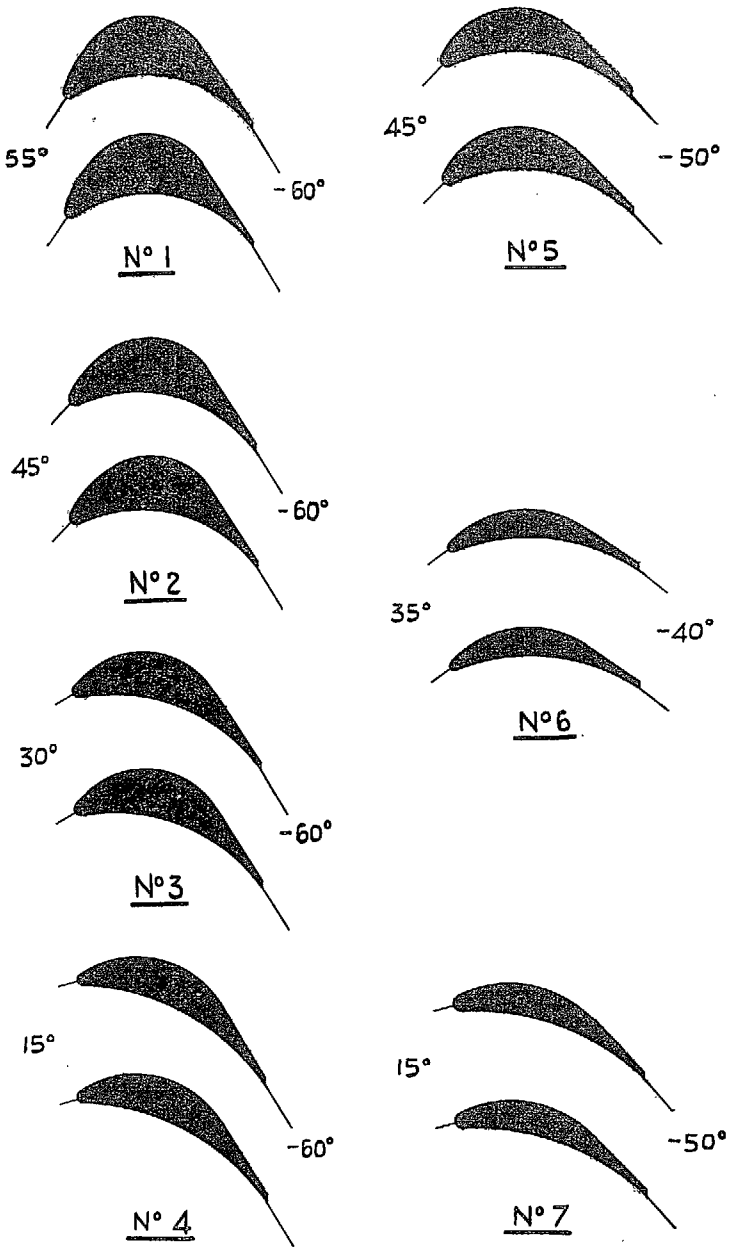

FIG. 5. Cascade details. Pitch/width = 0·625. Values of design inlet angles and $\cos^{-1}$ (throat/pitch) as indicated.

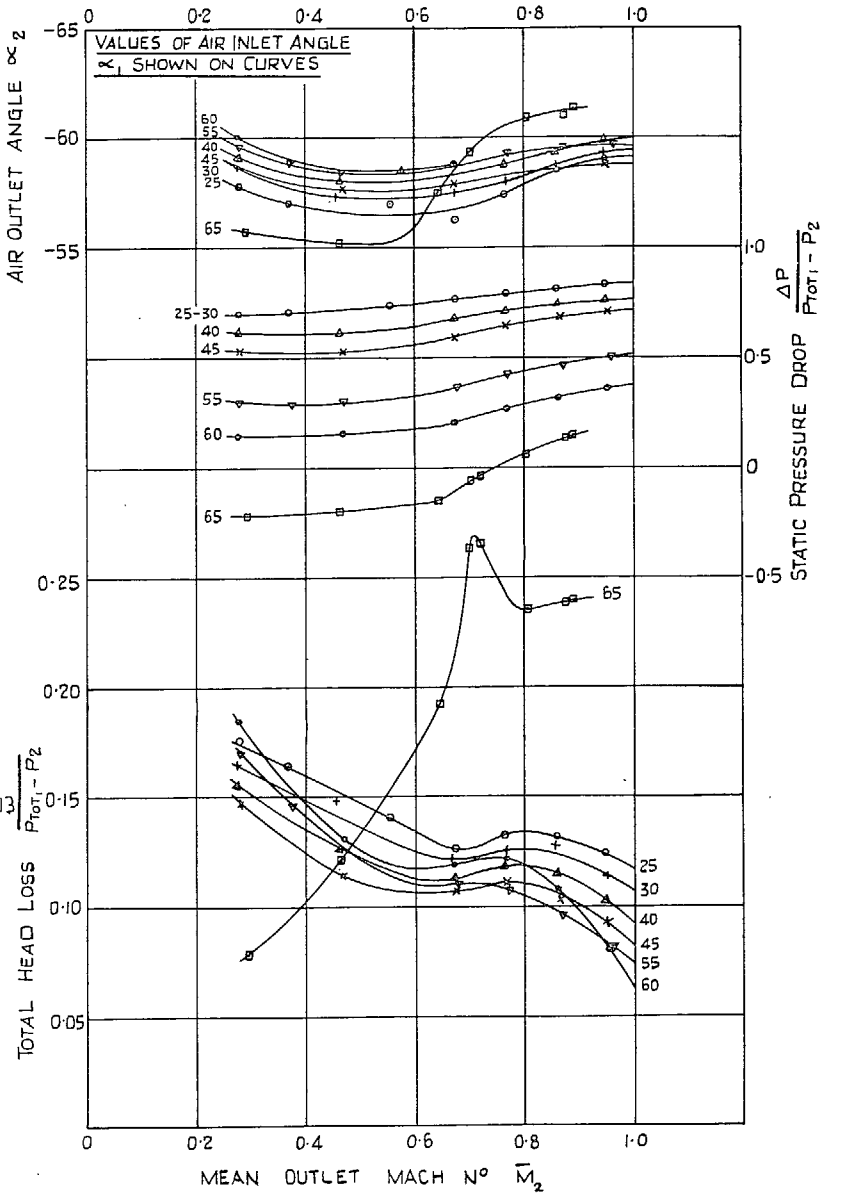

FIG. 6. Cascade No. 1. Design inlet angle 55 deg. $\cos^{-1}$ (throat/pitch) = — 60 deg.

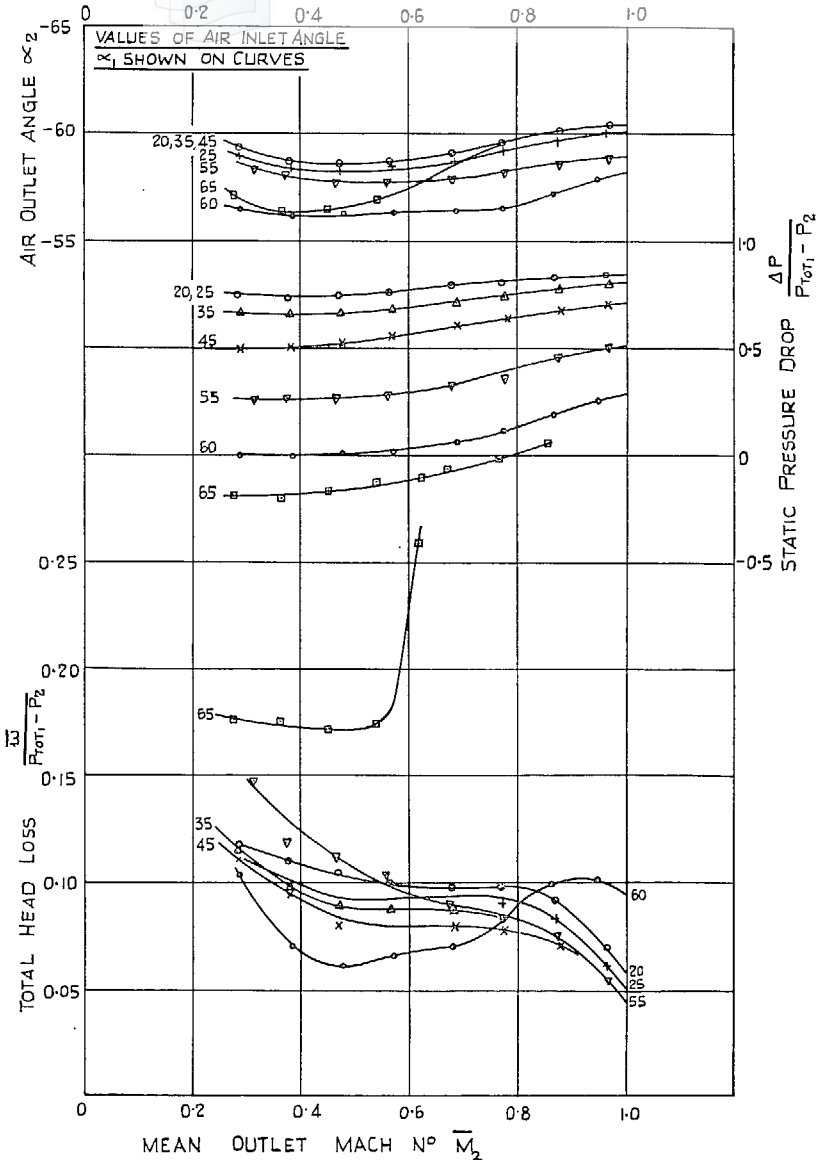

FIG. 7. Cascade No. 2. Design inlet angle 45 deg. Cos^{-1} (throat/pitch) = — 60 deg.

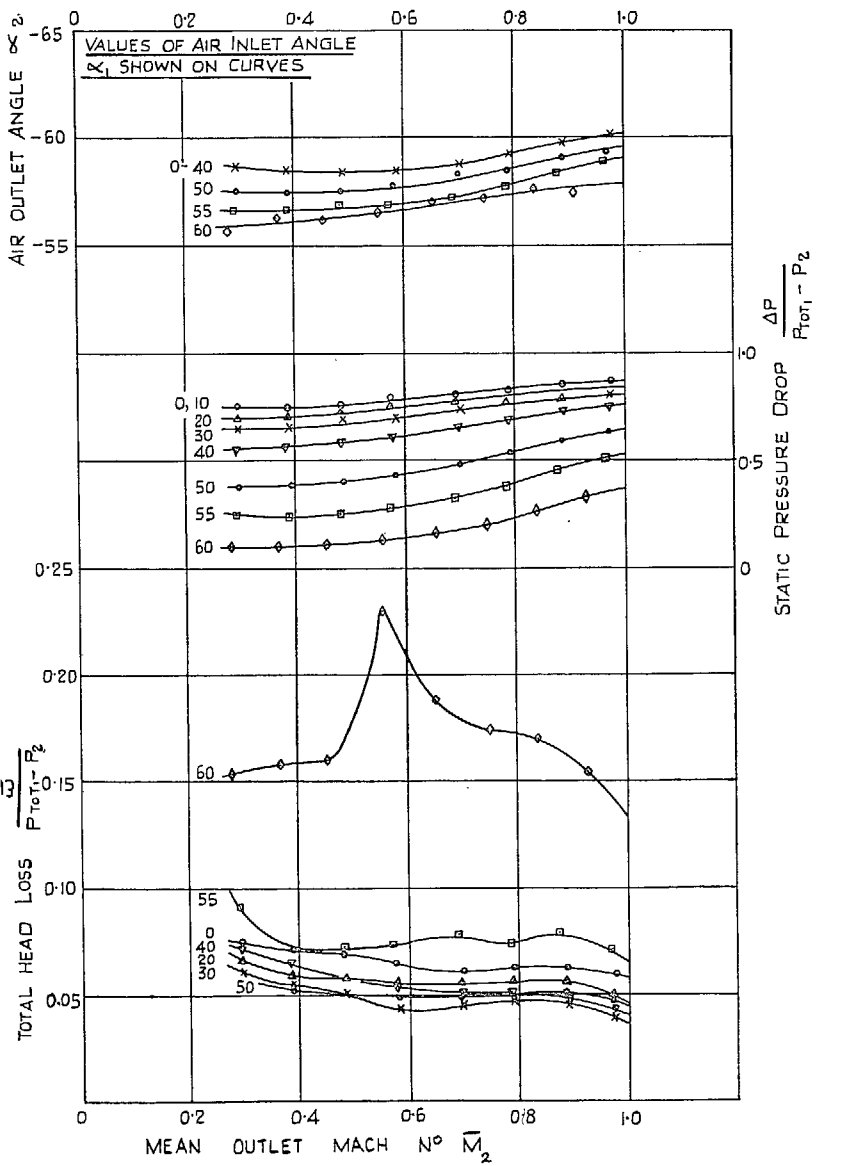

FIG. 8. Cascade No. 3. Design inlet angle 30 deg. Cos^{-1} (throat/pitch) = — 60 deg.

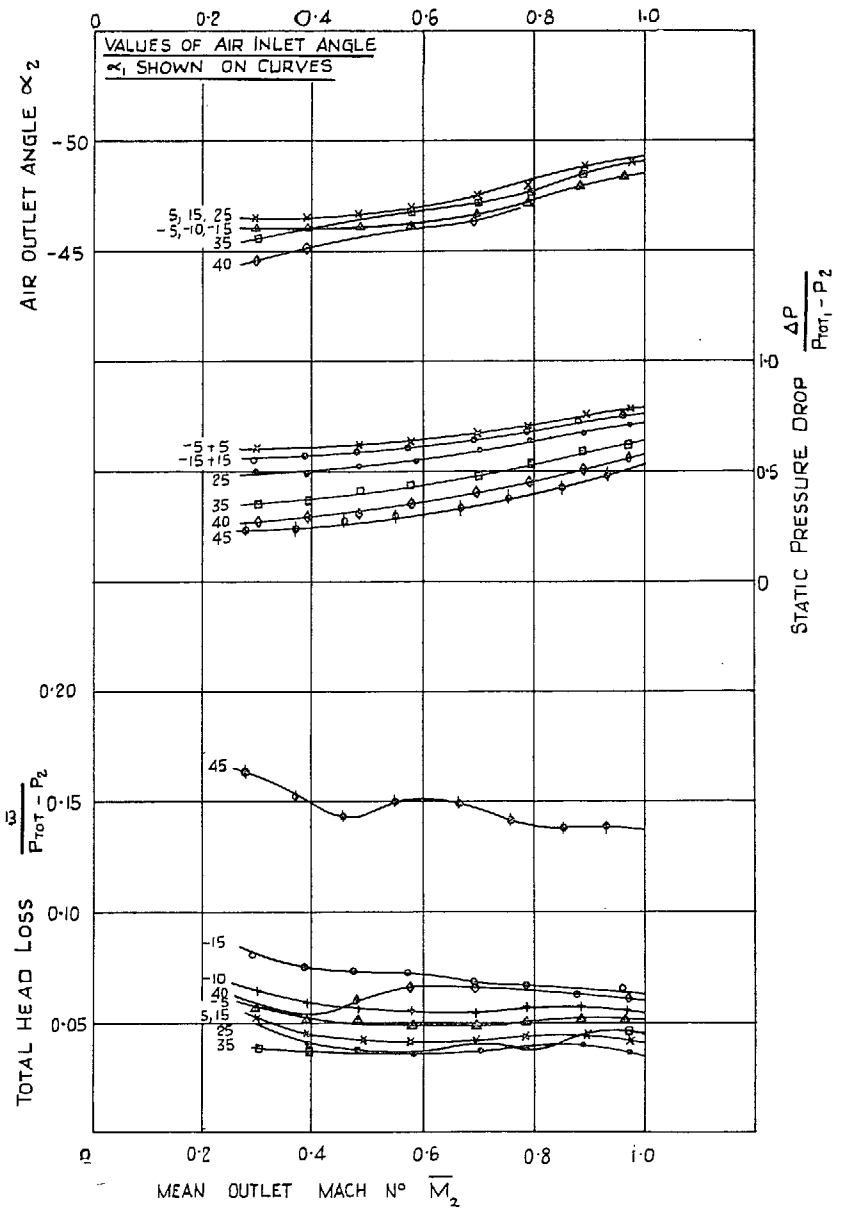

FIG. 9. Cascade No. 4. Design inlet angle 15 deg.
Cos^{-1} (throat/pitch) = — 60 deg.

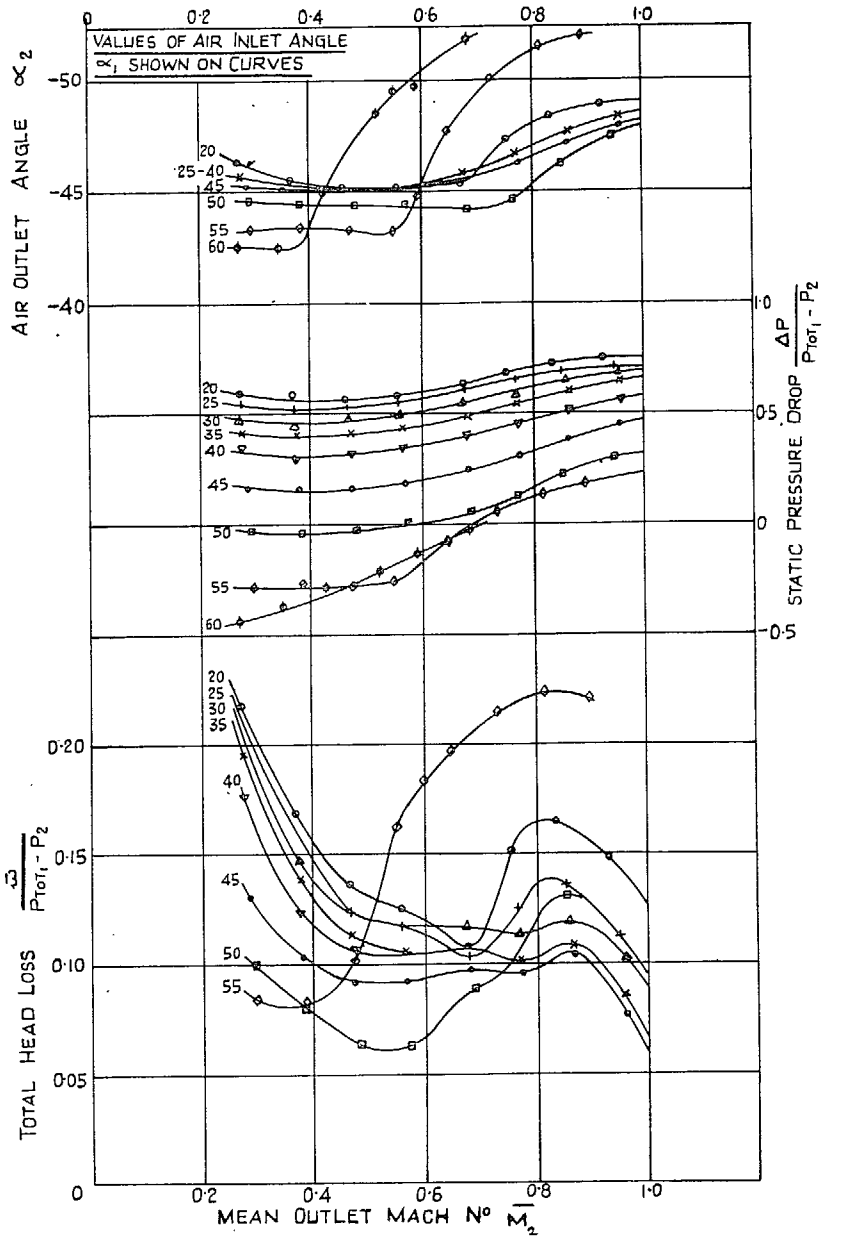

FIG. 10. Cascade No. 5. Design inlet angle 45 deg.
Cos^{-1} (throat/pitch) = — 50 deg.

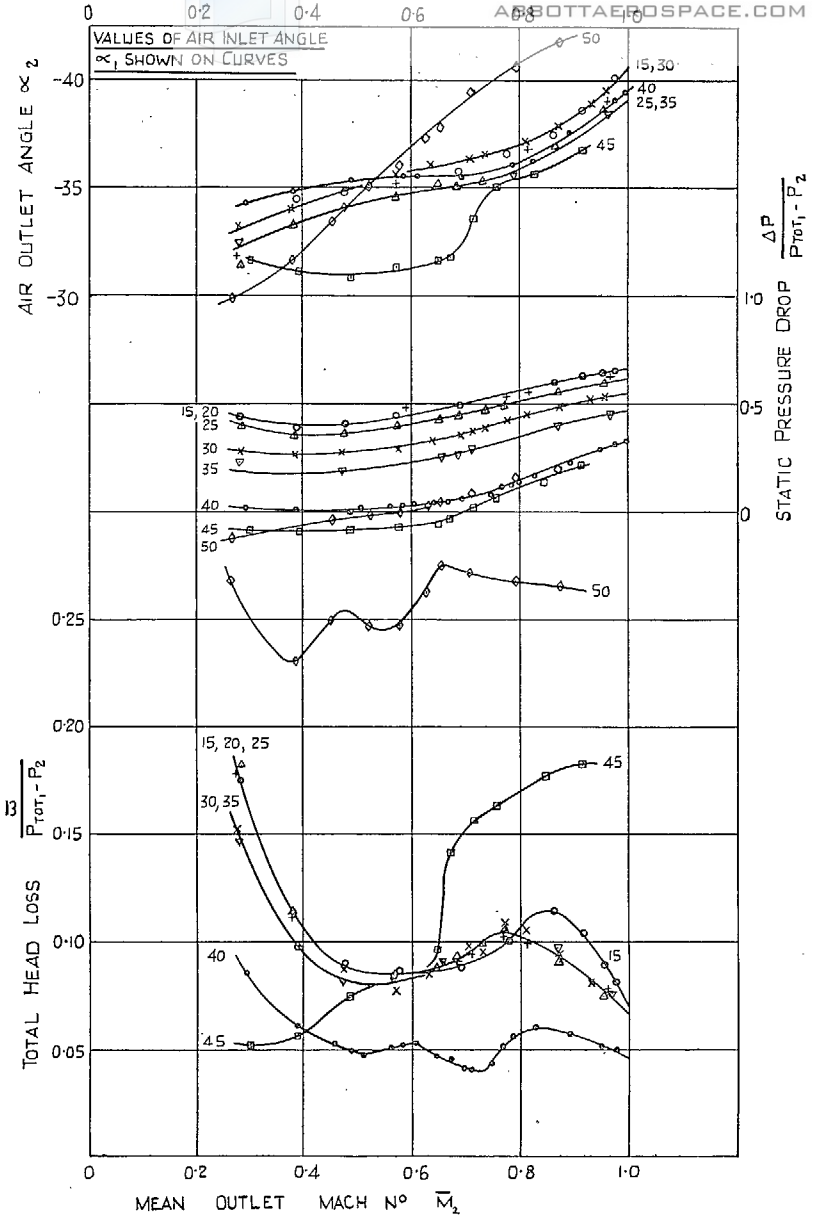

FIG. 11. Cascade No. 6. Design inlet angle 35 deg.
Cos^{-1} (throat/pitch) = — 40 deg.

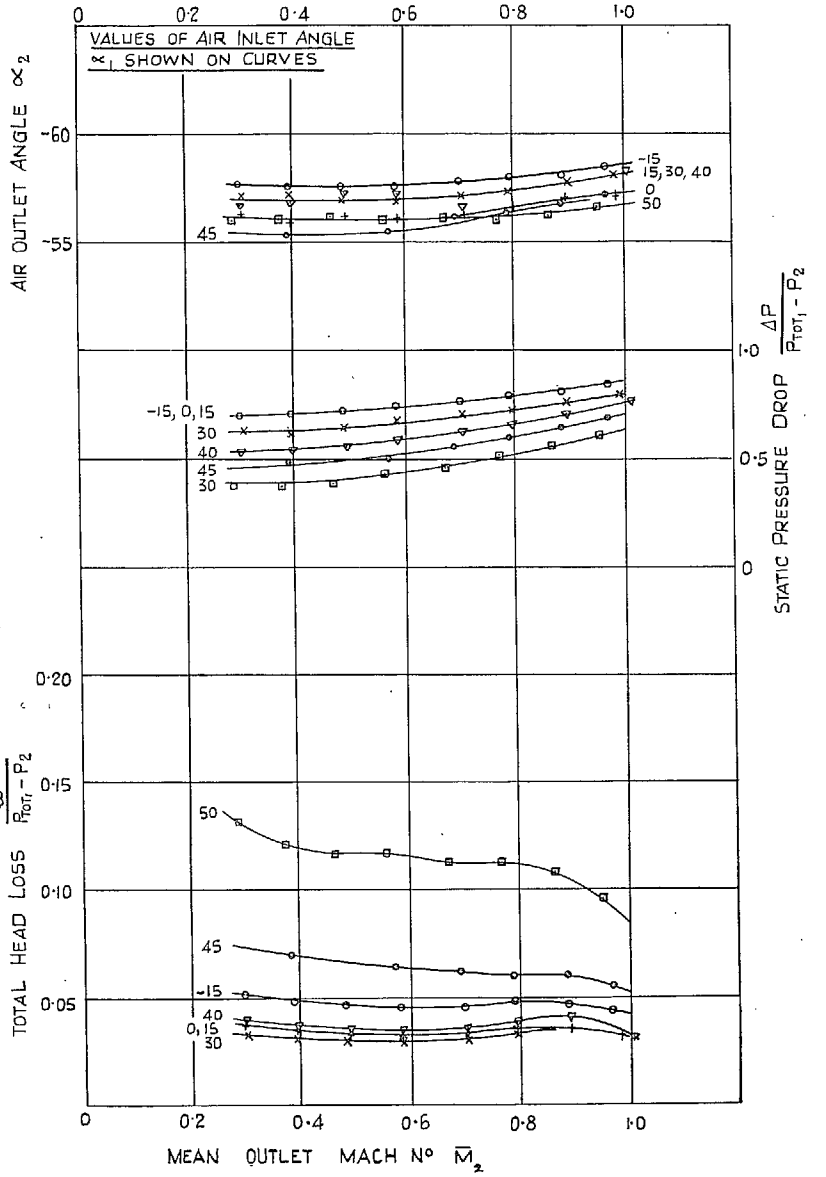

FIG. 12. Cascade No. 7. Design inlet angle 15 deg.
Cos^{-1} (throat/pitch) = — 50 deg.

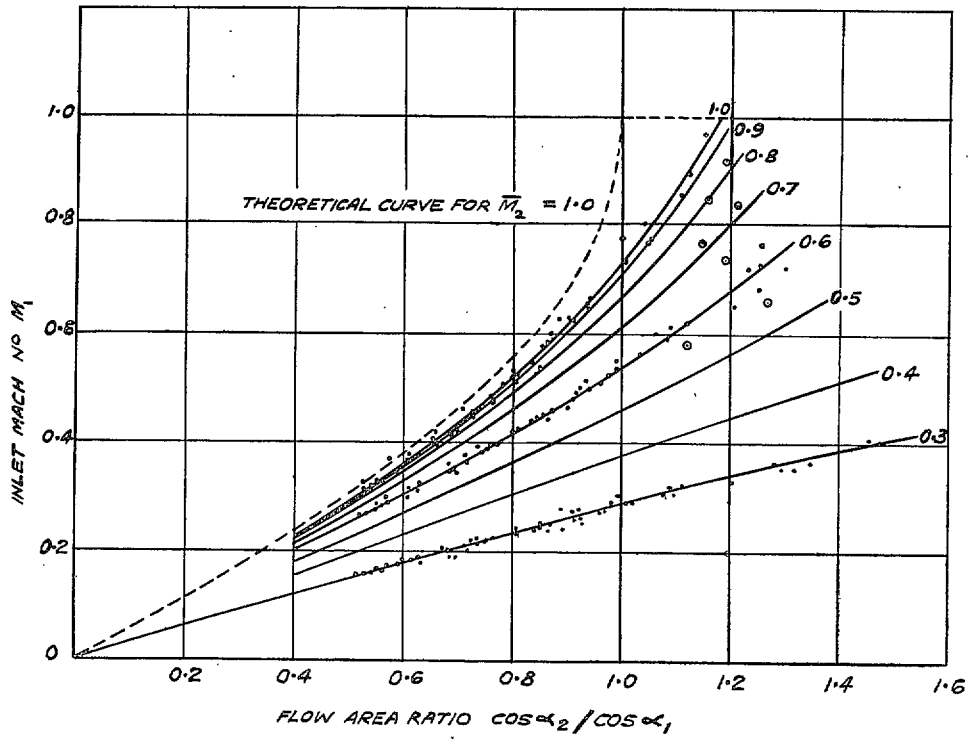

FIG. 13. Cascades Nos. 1 to 7. Values of mean outlet Mach number $\overline{M}_2$ shown on curves. Points shown thus —•— interpolated from test results for $\overline{M}_2 = 0{\cdot}3$, $0{\cdot}6$ and $1{\cdot}0$. Points shown thus · for impulse conditions, $\Delta P = 0$.

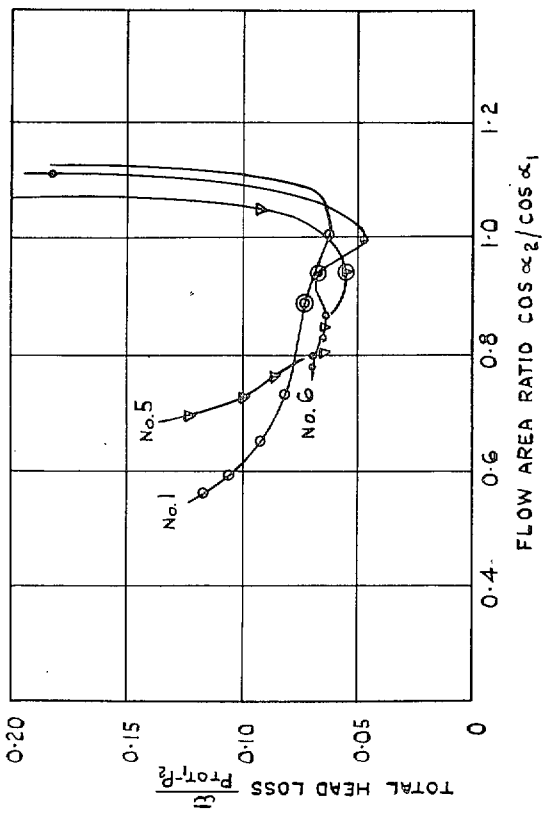

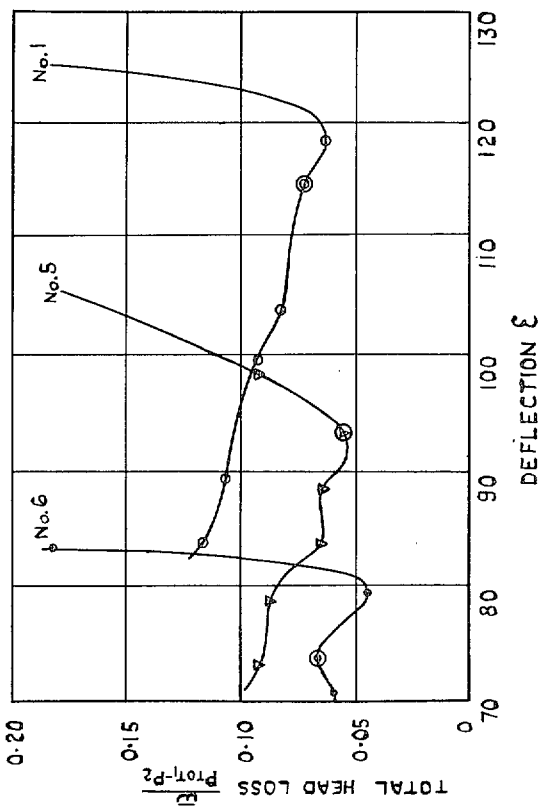

FIG. 14. Cascades Nos. 1, 5, 6. Design inlet angles 55, 45, 35 deg. Cos^{-1} (throat/pitch) = — 60, — 50, — 40 deg. Mean outlet Mach number $\overline{M}_2 = 1{\cdot}0$. Points of zero incidence are marked thus :—O.

(52305) Wt. 15/680 K.9 8/53 Hw PRINTED IN GREAT BRITAIN

Publications of the Aeronautical Research Council

ANNUAL TECHNICAL REPORTS OF THE AERONAUTICAL RESEARCH COUNCIL (BOUND VOLUMES)

1936 Vol. I. Aerodynamics General, Performance, Airscrews, Flutter and Spinning. 40*s.* (40*s.* 9*d.*)
Vol. II. Stability and Control, Structures, Seaplanes, Engines, etc. 50*s.* (50*s.* 10*d.*)

1937 Vol. I. Aerodynamics General, Performance, Airscrews, Flutter and Spinning. 40*s.* (40*s.* 10*d.*)
Vol. II. Stability and Control, Structures, Seaplanes, Engines, etc. 60*s.* (61*s.*)

1938 Vol. I. Aerodynamics General, Performance, Airscrews. 50*s.* (51*s.*)
Vol. II. Stability and Control, Flutter, Structures, Seaplanes, Wind Tunnels, Materials. 30*s.* (30*s.* 9*d.*)

1939 Vol. I. Aerodynamics General, Performance, Airscrews, Engines. 50*s.* (50*s.* 11*d.*)
Vol. II. Stability and Control, Flutter and Vibration, Instruments, Structures, Seaplanes, etc. 63*s.* (64*s.* 2*d.*)

1940 Aero and Hydrodynamics, Aerofoils, Airscrews, Engines, Flutter, Icing, Stability and Control, Structures, and a miscellaneous section. 50*s.* (51*s.*)

1941 Aero and Hydrodynamics, Aerofoils, Airscrews, Engines, Flutter, Stability and Control, Structures. 63*s.* (64*s.* 2*d.*)

1942 Vol. I. Aero and Hydrodynamics, Aerofoils, Airscrews, Engines. 75*s.* (76*s.* 3*d.*)
Vol. II. Noise, Parachutes, Stability and Control, Structures, Vibration, Wind Tunnels 47*s.* 6*d.* (48*s.* 5*d.*)

1943 Vol. I. (*In the press.*)
Vol. II. (*In the press.*)

ANNUAL REPORTS OF THE AERONAUTICAL RESEARCH COUNCIL—

1933–34	1*s.* 6*d.* (1*s.* 8*d.*)	1937	2*s.* (2*s.* 2*d.*)
1934–35	1*s.* 6*d.* (1*s.* 8*d.*)	1938	1*s.* 6*d.* (1*s.* 8*d.*)
April 1, 1935 to Dec. 31, 1936.	4*s.* (4*s.* 4*d.*)	1939–48	3*s.* (3*s.* 2*d.*)

INDEX TO ALL REPORTS AND MEMORANDA PUBLISHED IN THE ANNUAL TECHNICAL REPORTS, AND SEPARATELY—

April, 1950 - - - - R. & M. No. 2600. 2*s.* 6*d.* (2*s.* 7½*d.*)

AUTHOR INDEX TO ALL REPORTS AND MEMORANDA OF THE AERONAUTICAL RESEARCH COUNCIL—

1909–1949. R. & M. No. 2570. 15*s.* (15*s.* 3*d.*)

INDEXES TO THE TECHNICAL REPORTS OF THE AERONAUTICAL RESEARCH COUNCIL—

December 1, 1936 — June 30, 1939.	R. & M. No. 1850.	1*s.* 3*d.* (1*s.* 4½*d.*)
July 1, 1939 — June 30, 1945.	R. & M. No. 1950.	1*s.* (1*s.* 1½*d.*)
July 1, 1945 — June 30, 1946.	R. & M. No. 2050.	1*s.* (1*s.* 1½*d.*)
July 1, 1946 — December 31, 1946.	R. & M. No. 2150.	1*s.* 3*d.* (1*s.* 4½*d.*)
January 1, 1947 — June 30, 1947.	R. & M. No. 2250.	1*s.* 3*d* (1*s.* 4½*d.*)
July, 1951.	R. & M. No. 2350.	1*s.* 9*d.* (1*s.* 10½*d.*)

Prices in brackets include postage.

Obtainable from

HER MAJESTY'S STATIONERY OFFICE

York House, Kingsway, London, W.C.2; 423 Oxford Street, London, W.1 (Post Orders: P.O. Box 569, London, S.E.1); 13a Castle Street, Edinburgh 2; 39, King Street, Manchester, 2; 2 Edmund Street, Birmingham 3; 1 St. Andrew's Crescent, Cardiff; Tower Lane, Bristol 1; 80 Chichester Street, Belfast, or through any bookseller